IEEE 802.11n: On Performance of Channel Estimation Schemes over OFDM MIMO Spatially-Correlated Frequency Selective Fading TGn Channels

Roger Pierre Fabris Hoefel

***Abstract*—In this paper, we investigate the performance of Least Square (LS), Time Delay Truncation (TDT) and Model-Based (MB) channel estimation schemes specially designed to operate in a orthogonal frequency division multiplexing (OFDM) multiple input multiple output (MIMO) IEEE 802.11n system. We conclude, founded on analytical and simulation results over spatially correlated frequency selective TGn channels, that the TDT scheme presents the best performance in low signal-to-noise ratio (SNR) regime, whereas the performance of the LS scheme outperforms substantially the TDT and MB channel estimation schemes in high SNR regime.**

***Keywords*—802.11n; MIMO, OFDM; channel estimation**

I. INTRODUCTION

The process of development of the IEEE 802.11n amendment began in 2003 [1]. At the beginning of 2005 there were two main draft proposals: *(1)* one proposal was supported by the WWSE (World Wide Spectrum Efficiency), which was developed by companies like Broadcom, Motorola and Texas Instruments; (2) a second proposal was issued by the TGn Synch Group, which was supported by companies like Intel, Cisco, and Sony. Both draft proposals included spatial division multiplexing (SDM) up to four layers. The WWSE and TGn Synch teams suggested a bandwidth of 20 MHz and 40 MHz, respectively. There were also other differences concerning channel coding, interleaving and channel estimation schemes. These proposals were joined in 2006, given the origin of the Joint Proposal. Finally, the IEEE 802.11 amendment [2] was ratified in late 2009.

The IEEE 802.11n amendment supports a maximum gross physical (PHY) layer data rate of 260 Mbps [3, p. 100] and 540 Mbps [3, p. 140] within 20 MHz and 40 MHz bandwidth, respectively, when it is implemented orthogonal frequency division multiplexing (OFDM) multiple input multiple output (MIMO) SDM transmission scheme with four layers. The forward error correcting (FEC) scheme is based on the binary convolutional code (BCC) with frequency interleaving per OFDM symbol. The implementation of Low-Density Parity Code (LDPC) FEC scheme is optional.

We have designed a joint time-frequency synchronization scheme suitable for the OFDM MIMO IEEE 802.11n amendment [4]. The system performance was analyzed using a spatially multiplexing MIMO (SM-MIMO) architecture with either zero forcing (ZF) or minimum mean squared error (MMSE) linear receivers. We have concluded that for high cardinality modulation schemes is fundamental to improve the SDM-MIMO 802.11n performance using advanced transceiver architectures.

The performance of OFDM MIMO receivers is strongly dependent on the channel estimation accuracy. Therefore, in this paper, we shall analyze in great detail the impact of channel estimation schemes on the performance of IEEE 802.1n systems. To accomplish our targets the remaining of this paper is organized as follows. Section II summarizes previous works in this field in order to contextualize the contributions and relevance of this paper. Section III presents the channel estimation schemes analyzed in this paper. Section IV briefly describes the TGn channel models. Performance simulation of Least Square (LS), Time Delay Truncation (TDT) and Model Based (MB) channel estimation schemes in IEEE 802.11n systems is carried out in Section V. This section also presents a validation of the simulation results, a fundamental issue to reproducibility and credibility of the results shown in this paper. Finally, our conclusions are drawn in Section VI.

II. PREVIOUS WORKS AND RELEVANCE

A MIMO OFDM channel estimation scheme designed to operate in low signal-to-noise ratio (SNR) regime, the Time Domain Truncation scheme, was proposed in [5]. An orthogonal cover matrix (OCM) allowing that the training symbols used to MIMO channel estimation be transmitted in all antennas was also proposed in this paper. The performance of the TDT scheme was analyzed by simulation of a generic OFDM MIMO system.

The existence of null subcarriers in the preamble degrades the performance of the TDT scheme in the region with high SNR. A scheme to cope with this drawback, the Model-Based scheme, was proposed in [6]. The authors presented simulation and analytical results of the symbol error rate (SER) for M-ary phase-shift keying (MPSK) modulation assuming an OFDM single input single output (SISO) system over Rayleigh fading channels.

Comparative performance analysis between LS, TDT and MB channel estimation schemes was carried out in [7] by simulation of the IEEE 802.11n TGn Sync Draft amendment. The final version of the 802.11n amendment specifies the use of OCM (described in Section III) to transmit the MIMO channel estimation symbols. However, in the TGn Sync Draft the transmit antennas are driven one at a time for each subcarrier during the transmission of the reference symbols at the training period [7]. Therefore, the simulation results shown in [7] cannot be applied directly to the IEEE 802.11n amendment. One of the contributions of our paper is to investigate the performance of LS, TDT and MB channel estimation schemes using an IEEE 802.11n simulator that follows the ratified amendment. We also present a comparison between analytical and simulation results that validate the results shown in this paper. Finally, the established conclusions may be useful for future research activities in order to optimize the IEEE 802.11n system performance.

III. IEEE 802.11N: CHANNEL ESTIMATION SCHEMES

In this section, we first present a brief description of the IEEE 802.11n high throughput (HT) mixed format (MF) packet structure

Roger Pierre Fabris Hoefel, Department of Electrical Engineering, Federal University of Rio Grande do Sul (UFRGS), Porto Alegre, Rio Grande do Sul (RS), Brazil; E-mail: roger.hoefel@ufrgs.br.

for networks that operate in the 20 MHz bandwidth (see Fig. 1). After establishing a common background, we describe three different channel estimation schemes: Least-Square [8, p. 190]; Time Domain Truncation [5]; and Model-Based [6-7].

The legacy preamble allows that the 802.11a/g legacy devices can decode the legacy signal field (L-SIG), which transports control information about the current HT packet transmission in a format that can be decoded by all legacy devices. The legacy short training field (L-STF) carries ten repetitions of a short symbol used to packet detection, automatic gain control (AGC) and gross time and frequency synchronization. The L-LTF contains two long symbols, where each OFDM symbols is prepended with a cyclic prefix (CP). These symbols are used for fine time and frequency synchronization. The L-LTF is also used for channel estimation, which is necessary to decode the L-SIG and the HT-SIG control fields. The HT-SIG field contains two control OFDM symbols with CP each one, where the control information necessary to decode the data payload is transported, such as, payload length, modulation coding scheme (MCS) and transceiver architecture. The HT-STF is necessary to redo the AGC for MIMO operation. The HT-LTF contains symbols to MIMO channel estimation, where the number of HT-LTF symbols depends on the number of spatial streams transmitted [3, p. 280]. Finally, the data field contains OFDM symbols from the inverse Discrete Fourier Transform (IDFT) of the orthogonal subcarriers that transport the information data and pilot symbols. Note that each *3.2 μs* OFDM symbols has a CP of *800 ns*, which is added to make the system robust against inter-symbol interference (ISI) and inter-carrier interference (ICI). The 802.11n has 64 subcarriers for the 20 MHz bandwidth operation, where 52 subcarriers are used for data transmission, four subcarriers contain pilots to track the residual phase due to both imperfect time-frequency synchronization and channel estimation, one direct current (DC) null carrier, and seven subcarriers are used as guard band.

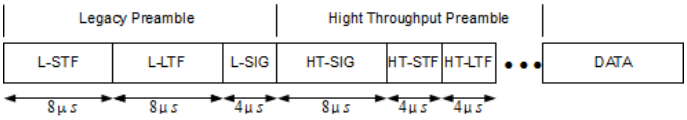

Fig. 1. HT-MF packet structure for 20 MHz bandwidth.

The L-LTF transports the same sequence in all transmit antennas using a cyclic shift diversity scheme (CSD), necessary to avoid undesirable beamforming effects since the control information transported by the L-SIG and HT-SIG fields must be decoded by all devices in the basic service set (BSS). Therefore, this field only allows channel estimation to implement a maximum ratio combiner (MRC) receiver, necessary to improve the reception of the L-SIG and HT-SIG control fields. On the other hand, the HT-LTF is specially designed to allow MIMO channel estimation.

The 802.11n amendment implements block type pilot structure since the HT-LTF OFDM symbols transmit training symbols across all 56 used subcarriers. In general, the channel is quasi-static due to both typical indoor usage models and usual packet lengths. The HT-LTF OFDM symbols transmit the following pattern across the subcarriers:

$$HTLT_{-28,28} = \begin{bmatrix} 1,1,1,1,-1,-1,1,1,-1,1,-1,1,1,1,1,1,1,-1, \\ -1,1,1,-1,1,-1,1,1,1,1,1,0,1,-1,-1,1,1,-1,1,-1,1 \\ -1,-1,-1,-1,-1,1,1,-1,-1,1,-1,1,-1,1,-1,1,1,1,1,1,-1,-1 \end{bmatrix}. \quad (1)$$

The time domain waveform for the *n*th HT-LTF ($1 \le n \le N_{SS}$) at each spatial stream i_{SS} is given by [3, p. 83]

$$r_{HT-LTF}^{n,i_{ss}} = \sqrt{\frac{1}{N_{SS} \cdot 56}} \sum_{k=-28}^{28} [P_{HLTF}]_{i_{ss},n} HLTF_k exp\left(j2\pi k\Delta f\left(t - T_{GI} - T_{CS}^{i_{SS}}\right)\right), \quad (2)$$

where N_{SS} is the number of spatial streams (SS); the subcarrier spacing is $\Delta f = 312.5\ kHz\ (20MHz/64)$; T_{GI} is the guard interval length; and $T_{CS}^{i_{SS}}$ denotes the CS for the SS i_{ss}. The orthogonal cover matrix (OCM) is given by (3). The number of transmitted HT-LTF OFDM symbols is given by (4). Finally, notice that an *800 ns* CP is prepended to each *3.2μs* OFDM symbol.

$$P_{HTLTF} = \begin{bmatrix} +1 & -1 & +1 & +1 \\ +1 & +1 & -1 & +1 \\ +1 & +1 & +1 & -1 \\ -1 & +1 & +1 & +1 \end{bmatrix} \quad (3); \quad N_{LTF} = \begin{cases} N_{SS} & if\ N_{SS} = 1,2,4 \\ 4 & if\ N_{SS} = 3 \end{cases} \quad (4)$$

A. Least-Square (LS) Channel Estimation

The 802.11n receiver, after removing the CP, performs the Discrete Fourier Transform (DFT) of each *3.2μs* HT-LTF OFDM symbol to obtain the training subcarriers. Hence, the observed training signal for the *k*th subcarrier at the DFT output is given by [3, p. 95]

$$\left[\boldsymbol{Y}_{t_1}^{(k)}, \boldsymbol{Y}_{t_2}^{(k)}, \cdots \boldsymbol{Y}_{N_{LTF}}^{(k)}\right] = \begin{bmatrix} \tilde{h}_{11}^{(k)} & \tilde{h}_{12}^{(k)} & \cdots & \tilde{h}_{1N_{SS}}^{(k)} \\ \tilde{h}_{21}^{(k)} & \tilde{h}_{22}^{(k)} & & \tilde{h}_{2N_{SS}}^{(k)} \\ \vdots & & \ddots & \vdots \\ \tilde{h}_{N_{RX}1}^{(k)} & \tilde{h}_{N_{RX}2}^{(k)} & \cdots & \tilde{h}_{N_{RX}N_{SS}}^{(k)} \end{bmatrix} \cdot \mathbf{P_{HTLF}} \cdot \mathrm{HTLF_k} + \left[\boldsymbol{Z}_{t_1}^{(k)}, \boldsymbol{Z}_{t_2}^{(k)}, \cdots \boldsymbol{Z}_{N_{LTF}}^{(k)}\right]. \quad (5)$$

where $\boldsymbol{Y}_{t_m}^{(k)}$ is a column vector of dimension N_{RX} that contains the received signal for the *n*th HT-LTF in the *k*th subcarrier at each receive antenna ($i=1,\ldots,N_{RX}$). The frequency response between the *i*th receive antenna and the *j*th transmit antenna for the *k*th subcarrier is denoted by $\tilde{h}_{ij}^{k}$, where the superscript till is used to indicate that the effects of CS, imperfect time and frequency synchronization are included in the observed channel response in the frequency domain. The noise column vector for the *n*th HT-LTF at *k*th subcarrier $\boldsymbol{Z}_{t_n}^{(k)} = \left[\boldsymbol{Z}_{t_1}^{(k)}, \boldsymbol{Z}_{t_2}^{(k)}, \cdots \boldsymbol{Z}_{N_{LTF}}^{(k)}\right]^{\boldsymbol{T}}$ is assumed to be zero-mean circular symmetric complex Gaussian (ZMCSCG) with variance N_0.

The OCM P_{HTLF} is unitary (i.e., $\boldsymbol{P}_{HTLTF} \cdot \boldsymbol{P}_{HTLF}^{T} = \boldsymbol{I}_{N_{SS}}$, where the $(.)^T$ indicates the transpose operation. Hence, using (5) and eliminating the null DC subcarrier, the normalized channel estimation matrix impaired with noise for the *k*th subcarrier can be obtained as follows [3, p. 96]:

$$\begin{bmatrix} \hat{h}_{11}^{(k)} & \hat{h}_{12}^{(k)} & \cdots & \hat{h}_{1N_{SS}}^{(k)} \\ \hat{h}_{21}^{(k)} & \hat{h}_{22}^{(k)} & & \hat{h}_{2N_{SS}}^{(k)} \\ \vdots & & \ddots & \vdots \\ \hat{h}_{N_{RX}1}^{(k)} & \hat{h}_{N_{RX}2}^{(k)} & \cdots & \hat{h}_{N_{RX}N_{SS}}^{(k)} \end{bmatrix} = \left[\boldsymbol{Y}_{t_1}^{(k)}, \boldsymbol{Y}_{t_2}^{(k)}, \cdots \boldsymbol{Y}_{N_{LTF}}^{(k)}\right]. P_{HTLF}^{T} \cdot \frac{1}{\mathrm{HTLF_k} \cdot \mathrm{N_{LTF}}} \quad (6)$$

It can be proved that (6) provides the LS solution of the observed channel frequency response since it minimizes for the *k*th subcarrier the following cost function [8, p. 190]:

$$J\left(\tilde{\boldsymbol{H}}^{(k)}\right) = \left\|\boldsymbol{Y}^{(k)} - \boldsymbol{H}^{(k)} \cdot \mathrm{HTLF_k}\right\|^2. \quad (7)$$

B. Time-Domain Truncation (TDT) Channel Estimation

The LS scheme demands the estimation of the frequency response for 56 out of 64 subcarriers. The TDT scheme is founded on the observation that in indoor environments the number of taps with significant power in the time domain impulsive response can be significantly lower than the DFT length [5]. Therefore, the truncation of the non-significant terms of the impulsive response can reduce the noise effects in environments with low delay spread and low SNR.

The TDT channel estimation algorithm is described as follows:

1. Calculate the LS solution of channel response in the frequency domain using (6) for the *subcarriers {k=-28,⋯,-1,+1,⋯,+28}*.

2. Determine the values for the subcarriers *{k = -32, -31,-30, -29, 0, 29, 30, 31}*. There are two basic approaches to accomplish it: *(i)* to use null values; *(ii)* to perform interpolation.

3. Determine the response impulsive in the time domain between the *i*th transmit antenna and the *j*th receive antenna:

$$\tilde{h}_{ij}[n] = IDFT_{64}\{\tilde{H}_{ij}\}, i = 1, \cdots N_{RX}, j = 1, \cdots, N_{TX}. \quad (8)$$

4. The channel impulsive is truncated in *L* samples according with the root mean square (rms) delay spread of the channel:

$$\hat{h}_{ij}[n] = \begin{cases} \tilde{h}_{ij}[n], & n = 0,1, \cdots, L \\ 0 & othewise \end{cases}. \quad (9)$$

5. The channel response in the frequency domain is given by

$$\hat{\boldsymbol{H}}_{ij} = DFT_{64}\{\hat{h}_{ij}[n]\}, i = 1, \cdots N_{RX}, j = 1, \cdots, N_{TX}. \quad (10)$$

C. Model-Based (MB) Channel Estimation

The TDT scheme needs to estimate the null carriers (cf. step 2) in order to estimate the impulsive response (cf. step 3). However, in the high SNR region, the estimation of null carriers can degrade minimum square error (MSE) of the channel estimation. The aim of the MB estimation scheme is to surpass the null carriers' drawback of the TDT scheme [6-7].

The MB channel estimation algorithm is described as follows [7]:

1. Perform the first four steps of the TDT channel estimation scheme.
2. Determine a Fourier Matrix **F** of dimension *56xL*.
3. Determine the frequency response correspondent to the truncated impulsive response as follows:

$$\bar{\bar{\boldsymbol{H}}}_{ij} = \boldsymbol{F} \cdot \hat{\boldsymbol{h}}_{\boldsymbol{ij}}, \quad (11)$$

where $\hat{\boldsymbol{h}}_{\boldsymbol{ij}}$ is a row vector with dimension *L* that contains the impulsive response estimated in (9).

5. Calculate the row vector with dimension *L*, $\bar{\bar{\boldsymbol{h}}}_{ij}$, which contains the impulsive response between the *i*th receive and *j*th transmit antenna:

$$\bar{\bar{\boldsymbol{h}}}_{ij} = [(\boldsymbol{F}^{\boldsymbol{H}}\boldsymbol{F})^{-1}\boldsymbol{F}^{\boldsymbol{H}}] \cdot \bar{\bar{\boldsymbol{H}}}_{\boldsymbol{ij}}, \quad (12)$$

where the superscript $(.)^H$ denotes Hermitian transpose operation. It can be proved that this impulse response is the LS criterion of (11).

6. Finally, the frequency response between the *i*th receive and *j*th transmit antenna is given by

$$\hat{\boldsymbol{H}}_{ij} = DFT_{64}\{\bar{\bar{\boldsymbol{h}}}_{ij}\}, i = 1, \cdots N_{RX}, j = 1, \cdots, N_{TX}. \quad (13)$$

IV. TGn Channel Models

The Task Group N (TGn) have specified six spatially correlated channel models [3, p. 52], [9]: TGn A (flat fading); TGn B (residential with maximum delay τ_{max} of *80 ns* and delay spread τ_{rms} of *15 ns*); TGn C (small office with τ_{max}=*200 ns* and τ_{rms}=*30 ns*); TGn D (typical office with τ_{max}=*390 ns* and τ_{rms}=*50 ns*); TGn E (multi-story office with τ_{max}=*730 ns* and τ_{rms}=*100 ns*); TGn F (large hotspot with τ_{max}=*1050 ns* and τ_{rms}=*150 ns*).

The TGn channels are based on the '*Kronocher model'*, as briefly described in the following [10-11]. The N_{RX} *x* N_{TX} correlated Rayleigh fading matrix **H,** which models the MIMO channel, is given by

$$vec(\boldsymbol{H}) = \boldsymbol{R}_H^{1/2} E\{vec(\boldsymbol{G})\}, \quad (14)$$

where *vec(.)* denotes the vector operation and $\boldsymbol{G}$ is a spatially white matrix of dimension N_{RX} *x* N_{TX}, whose entries are ZMCSCG random variable (rv) with unitary variance.

The correlation matrix of the MIMO N_{RX} *x* N_{TX} channel is a $(N_{RX} \cdot N_{TX}) \times (N_{RX} \cdot N_{TX})$ matrix given by

$$R_{\mathbf{H}} = E\{vec(\boldsymbol{H}) \cdot vec(\mathbf{H})^H\}, \quad (15)$$

The '*Kronocher model'* assumes that the joint spectrum of the Direction-of-Departure (DoD) and Direction-of-Arrival (DoA) are separable. Therefore, the correlation (15) can be rewritten as [11]

$$R_{\mathbf{H}} = \frac{1}{tr\{R_{\mathbf{H}}\}} \boldsymbol{R}_{TX} \otimes \boldsymbol{R}_{RX}, \quad (16)$$

where *tr{.}* and $\otimes$ denote the trace of matrix and the Kronecker product, respectively. $\boldsymbol{R}_{TX}$ and $\boldsymbol{R}_{RX}$ denote the transmit and receive correlation matrices.

The TGn channel models have impulse response based on the cluster model. Therefore, using the '*Kronocker model*', the channel matrix for the *m*th tap of *l*th cluster is given by

$$\mathbf{C_{m,l}} = \sqrt{\mathrm{P_{m,l}}} \cdot \sqrt{\mathbf{R}_{\mathrm{Rx,m,l}}} \cdot \mathbf{G} \cdot \left(\sqrt{\mathbf{R}_{\mathrm{TX,m,l}}}\right)^{\mathrm{T}}, \quad (17)$$

where $\sqrt{P_{m,l}}$ is the power for the *m*th tap of *l*th cluster. $\mathbf{R}_{\mathrm{RX,m,l}}$ and $\mathbf{R}_{\mathrm{TX,m,l}}$ denote the receive and transmit correlation matrices for the *m*th tap of *l*th cluster, respectively. In this paper, an underspread block fading channel is assumed, where the Doppler effects are neglected at each MF packet (i.e., a typical indoor scenario). The full details and parameters necessary to model the impulsive response of TGn channels A to F can be found in [9].

Figures 2 and 3 show the absolute value of the equivalent low-pass impulsive response for channels TGn B (maximum delay of *80 ns*) and F (maximum delay of *1050 ns*), respectively. These figures, although they are a single realization the MIMO 4x4 channel, depict graphically some design issues of MIMO transceivers in 802.11n systems, such as, they must be robust enough to cope with channels that present a large random variation of delay spread, number of taps, position of the tap with maximum power and so forth.

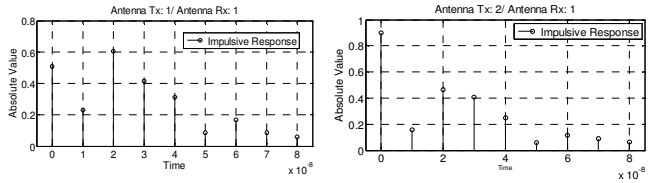

Fig. 2. Absolute value of typical baseband impulsive responses for the TGn B channel: (a) TX1/RX1; (b) TX 2/RX1. The abscissa axis scale is 10^{-8}.

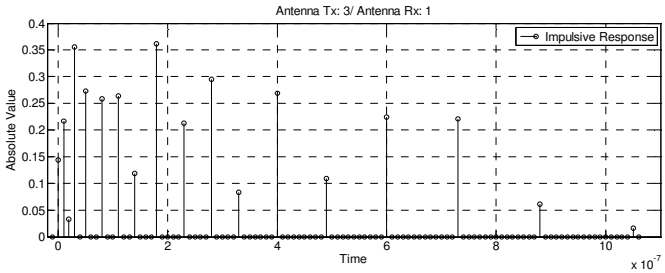

Fig. 3. Absolute value of a typical baseband impulsive response between the third transmit antenna and the first receive antenna for the MIMO 4x4 TGn F channel. The abscissa axis scale is 10^{-7}.

V. IEEE 802.11n: Performance Analyses

An *ipsis litteris* IEEE 802.11n and 802.11a/g PHY layer simulator has been developed using *Matlab* and ANSI *C* [12]. We also have performed an extensive comparison between simulation and analytical results in order to validate the core of the developed simulator [4, 12]. Therefore, we have tried to accomplish the fundamental issue of credibility, which is fundamental when the conclusions are strongly based on simulations results.

The SNR for the 802.11n OFDM MIMO system can be expressed as

$$SNR = \frac{E_b}{N_0}\left(\frac{N_{data}+N_{pilot}}{N_{FFT}}\right)(N_{BPSCS}\, r), \quad (18)$$

where E_b is the energy per bit and N_0 is the variance of ZMCSCG rv [12]. For a bandwidth *W* of 20 MHz, the remaining parameters are: Fast Fourier Transform length (N_{FFT}) of 64 samples; number of data subcarrier (N_{data}) equals to 52; number of pilot subcarriers (N_{pilot}) equals to 4; N_{BPSCS} is the number of bits per subcarrier per stream (i.e., the modulation cardinality*); r* denotes the code rate of the BCC.

The simulation results show in this paper assume a realist synchronization scheme [4] with no frequency offset impairment.

A. Mean Square Error (MSE) of the Channel Estimation

The MSE error of the channel estimation in 802.11n systems can be defined as

$$MSE = \mathrm{E}\left\{\sum_{\substack{k=-28\\k\neq 0}}^{28}\sum_{i=1}^{N_{RX}}\sum_{j=1}^{N_{TX}}\left|H_{ij}^{(k)} - \hat{H}_{ij}^{(k)}\right|^2\right\}, \quad (19)$$

where E[.] denotes expected value, $H_{ij}^{(k)}$ and $\hat{H}_{ij}^{(k)}$ are the ideal and estimated frequency response between *i*th receive and *j*th transmit antennas at *k*th subcarrier.

Fig. 4 shows the MSE of LS and TDT channel estimation schemes as function of the SNR for SISO TGn channels A, B, D and F. The performance of LS scheme is highly superior in relation to the TDT scheme in high SNR regime. Hence, the implementation of TDT scheme is feasible only in environments with low SNR, where the noise reduction due to the truncation of the impulsive response (cf. Eq. 9) compensates the distortion induced in the frequency response (cf. Eq. 10). These results also allow inferring the following conclusions: *(i)* the LS scheme is very robust since practically the same MSE is obtained for flat fading TGn A channel and highly frequency selective TGn D channel. However, a performance degradation is observed for the TGn F channel since its impulsive response is longer than the CP of *800 μs,* and, therefore, there is a residual ICI; *(ii)* the performance of TDT scheme presents a strong dependence with the number of samples of the impulsive response that are taken into account in Eq. (9). Note that the using the TDT scheme with L equals to 32 over the SISO TGn F channel reduces the MSE error in the high SNR region, but increases the MSE in the low SNR region in relation to the one obtained with the TDT scheme using *L=16*.

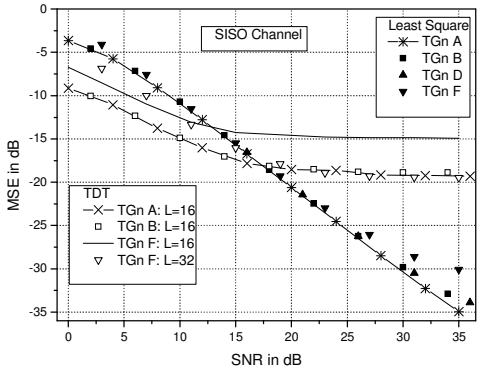

Fig. 4. MSE of channel estimation as a function of the SNR for TGn A, B, D and F over SISO channels using LS and TDT channel estimation schemes.

Fig. 5 shows the MSE of LS and MB channel estimation schemes as function of the SNR assuming MIMO 4x4 TGn channels A, B, and D. The fundamental conclusion is that the performance of LS scheme is highly superior in relation to the performance of the MB scheme for the whole SNR range. The performance of the MB channel estimation scheme depends strongly on the level of frequency selective of the channel as well as on the number of samples of the impulsive response that are taken into account. As observed for SISO channels, the performance of TDT scheme is also superior in relation to LS and MB channel estimation schemes for MIMO channels in the low SNR regime, but it degrades substantially the MSE in the high SNR region. Finally, comparing the results shown in Figs. 4 and 5 allow concluding that the performance of LS scheme is practically the same for SISO and MIMO 4x4 channels for the range of the SNR simulated.

Theoretically, the MSE error of LS estimation is given by

$$MSE_{LS} = \mathrm{E}\left[\left(\mathbf{H} - \hat{\mathbf{H}}\right)^{\mathrm{H}}\left(\mathbf{H} - \hat{\mathbf{H}}\right)\right] = \frac{1}{\mathrm{SNR}}, \quad (20)$$

where $\mathbf{H}$ and $\hat{\mathbf{H}}$ denote the ideal and estimated baseband complex MIMO channel matrices [3, p. 191]

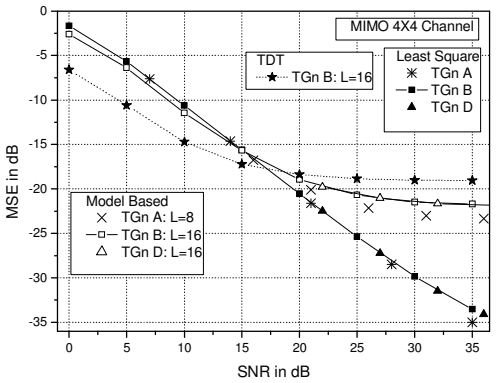

Fig. 5. MSE of channel estimation as a function of the SNR for TGn A, B and D MIMO 4x4 channels using LS, TDT and MB schemes.

Fig. 6 shows an excellent agreement between theoretical (straight line) and simulation results for the canonical MIMO 4x4 flat fading Rayleigh channel. For the TGn A channel (i.e., a flat fading channel with spatial correlation for both transmit and receive antennas) there is a minor discrepancy for high values of the SNR. There is a difference of approximately 2 dB between the analytical and simulation results over frequency selective TGn B and D channels when the SNR is equal to 40 dB. We also have observed that for TGn F channel there is a MSE floor around 30 dB. We have conjectured that the degradation of the MSE observed for TGn channels B, D and F happens because the 802.11n receivers use a sample period of *50 ns* (*1/W=1/20x10*^{6}), while the TGn channels are specified in intervals of 10 ns. Therefore, this can induce a floor on the attainable MSE at high SNR due to aliasing effects. Besides this characteristic, for the TGn F channel the CP of 800 ns is lower than the maximum delay of impulsive response of *1050 ns*, which causes ICI, and, therefore, in the strict sense there is a lack of complete correspondence between the circular convolutional use to estimate the channel and the linear convolutional that is used to determine the physical signal at the channel output. However, in the extremely competitive global broadband wireless market with low profit margins is not cost effective to design hardware to provide an SNR above 35 dB due to noise figure (NF) and other implementation impairments in the analog radio-frequency (RF) frontend and analog-to-digital converters (ADC) [3, p. 120]. Hence, the LS channel estimation scheme works accurately in the SNR operational range of practical IEEE 802.11n networks.

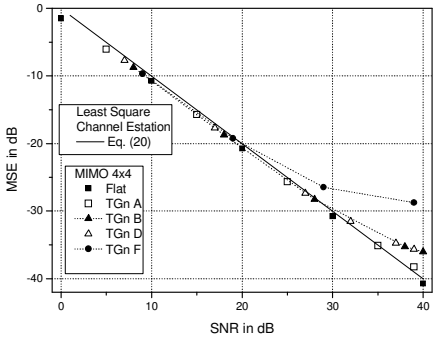

Fig. 6. MSE of channel estimation as a function of the SNR in dB for canonical MIMO 4x4 flat fading Rayleigh channel and TGn A, B, D and F MIMO 4x4 channels using LS channel estimation scheme.

The MSE results for the LS channel estimation scheme presented in [7] do not agree with the theoretical results given by (20) and ratified in this paper, as shown in Fig. 6. Probably, this discrepancy occurs because the authors in [7] considered all the subcarriers in MSE calculation (cf. Eq. 11 and Fig. 1 of [7]). In this paper, we have only considered the subcarriers that are effectively used for transmission

of data and pilot symbols (cf. Eq. 19). However, there is an agreement between our results and the results shown in [7] for the MB channel estimation scheme. This is not a paradox since one of advantages of the MB channel estimation scheme is to produce a better channel estimation in relation to LS scheme in the null subcarriers used for guard band and DC (see Section III).

Fig. 7 shows sample functions of the absolute value of the base band frequency response as a function of the subcarrier index for TGn B (left-side) and TGn D (right-side) MIMO 4x4 channels, while Fig. 8 shows the absolute value (right-side) and phase (left-side) in degrees for the MIMO 4x4 TGn F channel. These figures ratify the MSE results shown in Figures 4 and 5 since we can observe the close agreement between the real frequency response (blue lines) and the LS estimated channel frequency response (red crosses). These plots also clearly depict that the TGn channels model environments with both low frequency selectivity and high correlation among adjacent subcarriers (i.e., the TGn B channel) as well as radio environments with enormous frequency selectivity and low correlation among subcarriers (i.e., the TGn F channel).

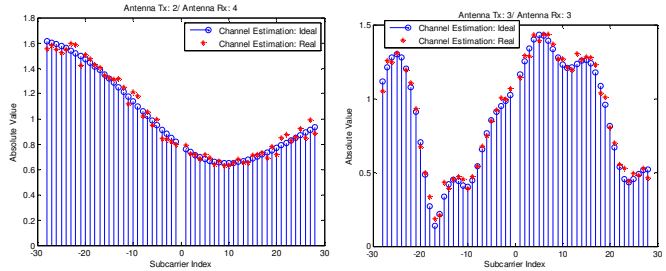

Fig. 7. Absolute value of the real (blue lines) and LS estimation (red crosses) frequency response sample function versus the subcarrier index for the MIMO 4x4 TGn B (left-side) and TGn D (right-side) channels with a SNR=25 dB.

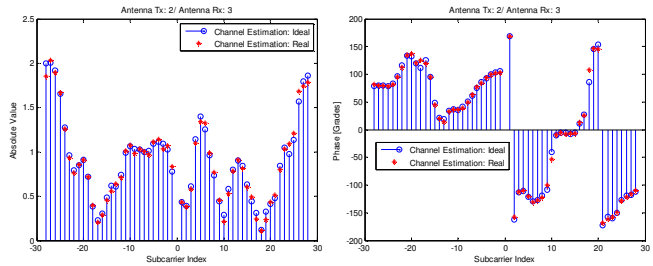

Fig. 8. Absolute value (right-side) and phase in degrees of the real (blue lines) and LS estimation (red crosses) frequency response sample function versus the subcarrier index for the MIMO 4x4 TGn F channel with a SNR=25 dB.

B. Effects of Channel Estimation on the MPDU PER

This subsection investigates the impact of the analyzed channel estimation schemes on the medium access control (MAC) protocol data unit (MPDU) packet error rate (PER). Hereafter, a payload length of 1024 bytes and soft-decision Viterbi decoding are assumed.

Fig. 9 shows the MPDU PER as a function of the SNR for the following configurations: *(1)* flat fading Rayleigh SISO channel using the MSC3 (Modulation Code Scheme 3: 16-QAM and BCC with code rate r=1/2); (*2*) MIMO 4x4 TGn D channel using MCS24 (BPSK, BCC with r=1/2); *(3)* MIMO 4x4 TGn D channel using MCS27 (16-QAM, BCC with r=1/2). Matched filter receiver (MF) is implemented in the simulated SISO environment, while the minimum mean squared error (MMSE) receiver is implemented over MIMO channels [12].

Analyzing the results for the SISO case, we can see that the analytical MPDU PER upper bound derived in [12] allows a reasonable estimation of the MPDU PER when it is compared with the simulation results obtained with perfect channel estimation. Note that for a PER of 1%, the realistic LS channel estimation scheme demands 1.5 dB more in relation to the perfect channel estimation scheme.

The simulation results for the MIMO 4x4 TGn D channel ratify the earlier conclusion that the TDT channel estimation scheme allows a superior performance in relation to the LS scheme in the low SNR region (see results for MCS24: BPSK, BCC with r=1/2). On the other hand, the performance of TDT channel estimation scheme degrades substantially at high SNR regime, where the LS channel estimation scheme works properly (see results for MCS27: 16-QAM, BCC with r=1/2).

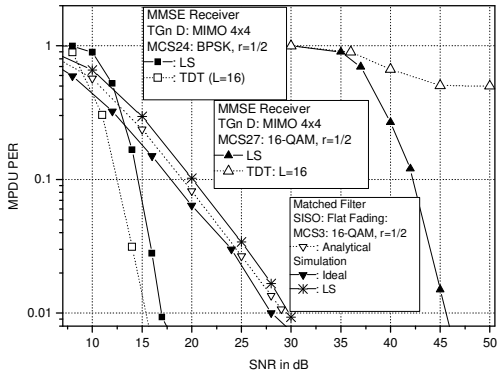

Fig. 9. MPDU PER as a function of the SNR in dB,

VI. CONCLUSIONS

In this paper, we described three different channel estimation schemes suitable to operate in IEEE 802.11n devices: the Least Square (LS); Time Delay Truncation (TDT) and Model-Based (MB). Founded on analytical and simulation results of the MMSE and MPDU PER, we have concluded that the TDT presents a superior performance in the low SNR regime, while the LS channel estimation schemes outperforms dramatically the other two schemes in the high SNR region. As a future research activity, we plan to develop tracking schemes to refine the estimate channel frequency response using the decision direct channel estimation paradigm.

REFERENCES

[1] T. Paul, T. Ogunfunmi, "Wireless LAN comes of age: Understanding the IEEE 802.11n amendment," in *Circuits and Systems Magazine,* First Quarter 2008, p. 28-54., 2008.

[2] Wireless LAN Medium Access Control (MAC) and Physical Layer) Specifications, Amendment 5: Enhancement for Higher Throughput. IEEE Std 802.11n-2009, 2009.

[3] E. Perahi, R. Stacey, Next Generation Wireless LANS. New York, USA: Cambridge University Press, 2008.

[4] R. P. F. Hoefel. "On the synchronization of IEEE 802.11n devices over frequency selective TGn channel models," *25th Annual Canadian Conference on Electrical and Computer Engineering (CCECE 2012),* Montreal, 2012

[5] A. N. Mody, G. L. Stuber, "Receiver implementation of a MIMO OFDM System," in *Proc. IEEE Global Telecommunications (Globecom), 2002.*

[6] X. Cai, G. H. Giannakis, "Error probability minimizing pilots for OFDM with M-PSK modulation over Rayleigh-fading channels," in *IEEE Transactions on Vehicular Technology,* vol. 53, pp. 146-155, Jan. 2004.

[7] I-Tai, Kun-Ju Tsai, "Channel estimation in a proposed IEEE 802.11n OFDM MIMO systems," in *2007 IEEE Sarnoff Symposium*, 2007.

[8] Y. S. Cho, J. Kim, W. Y. Yang and C. G. Kang, MIMO-OFDM Wireless Communications with MATLAB. Singapore: John Wiley & Sons, 2010.

[9] IEEE 802 11-03/161r2, *TGn* Indoor MIMO WLAN *Channel Models.*

[10] J. P. Kermoal et. al., "A stochastic MIMO radio channel model with experimental validation," in *IEEE Journal Select Areas on Communication*, vol. 20, pp. 1211-1226, Aug.2002.

[11] H. Ozcelik et. al., "Deficiencies of 'Kronecker' MIMO radio channel model," *in Electronics Letters*, vol. 29, no. 6, pp. 1209-1210, Aug. 2003.

[12] A. M. Câmara, R. P. F. Hoefel, "On the performance of IEEE 802.11n: analytical and simulations results," *in XXIX Brazilian Symposium of Telecommunications, SBrT 2011,* Curitiba, 2011.